THE JOURNAL OF BIOLOGICAL CHEMISTRY
Vol. 273, No. 48, Issue of November 27, pp. 32102–32110, 1998
© 1998 by The American Society for Biochemistry and Molecular Biology, Inc.
Printed in U.S.A.

Complexity of Trypanosomatid Endocytosis Pathways Revealed by Rab4 and Rab5 Isoforms in *Trypanosoma brucei**

(Received for publication, January 26, 1998, and in revised form, June 24, 1998)

Helen Field, Mariam Farjah, Arun Pal, Keith Gull‡, and Mark C. Field§

From the Laboratory of Cell Biology, Department of Biochemistry, Imperial College of Science, Technology and Medicine, Exhibition Road, London SW7 2AY, United Kingdom and the ‡School of Biological Sciences, University of Manchester, Stopford Building, Oxford Road, Manchester M13 9PT, United Kingdom

Small G proteins of the Rab family are responsible for vesicle fusion and control flux during intracellular transport. Rab5 is important in endosome maturation and Rab4 in recycling of endocytic material. Three Rab5 isoforms identified so far in mammals and three in the yeast genome suggest that conservation of multiple Rab5 isoforms is required for sophisticated regulation of endocytosis. *Trypanosoma brucei* homologues of Rab5 and Rab4 (TbRab5A and TbRab4) have been identified. Here we report cloning of a second Rab5 homologue, TbRab5Bp. The *TbRAB5A* and *-5B* genes are not linked in the genome, and phylogenetic reconstruction indicates that multiple Rab5 isoforms in yeast, mammals, and trypanosomes evolved independently. Northern blots demonstrate that TbRab5A, -5B, and TbRab4 messages are expressed in bloodstream form (BSF) and procyclic forms of the parasite even though endocytosis is not very active in the latter form. mRNA levels of TbRab5A and -4 are constitutive. Multiple-sized TbRab5B messages at very low abundance are detected, with greater expression in BSF. Also, the TbRab5B mRNA has a large 3′-untranslated region suggestive of potentially complex regulation, and therefore TbRab5Bp may be an important regulator of differential endocytosis levels between BSF and procyclic stage parasites. Affinity purified antibodies raised to C-terminal peptide sequences of all three TbRab proteins recognized small vesicular cytoplasmic structures, which for TbRab5Ap and -5Bp are predominantly near the flagellar pocket. TbRab5Bp colocalizes with invariant surface glycoprotein 100 (ISG_{100}), a protein entering the endocytotic pathway in BSF parasites, whereas in procyclic cells populations of vesicles stained with both TbRab5Ap and -5Bp substantially overlap; TbRab5 proteins are therefore components of the endocytotic pathway. TbRab4p localizes to vesicular structures throughout the cytoplasm, with some overlap with TbRab5Bp, but the majority occupying a different compartment to the TbRab5s. Therefore the trypanosome endosomal system has been functionally dissected for the first time; these reagents provide a unique opportunity for manipulation of the protozoan endosomal system to further our understanding of drug uptake mechanisms and virulence.

Rabs are a family of small GTPases essential for membrane vesicle trafficking in eukaryotes (1). Each Rab localizes to a distinct subset of organelles; the C terminus is responsible for intracellular localization (2), while the N terminus also recognizes the target organelle and is required for vesicle fusion (3). The Rab system controls organelle-specific flux by regulating the ability of the t- and v-SNARE partners to interact, promoting docking and fusion (4, 5). The amount of time that Rab5 remains GTP-bound governs the lifetime of the fusion-competent state of the docking vesicle (6).

Humans and yeast each have three identified Rab5 isoforms in the endosome system which colocalize, suggesting complex regulation or redundancy (7–10). Dominant negative Rab5 decreases endosome size, whereas constitutively active Rab5 leads to endosomal swelling and fusion (11). Phospholipase A_2 and phosphatidylinositol 3-kinase are implicated in Rab5 function (12, 13), suggesting close integration with signal transduction pathways. Rab4 is involved in recycling of membrane material back to the plasma membrane from endosomal compartments (14). Human Rab4a is subject to cell-cycle-dependent phosphorylation and is involved in insulin-mediated translocation of glucose transporters (15, 16). A second isoform, Rab4b, is not phosphorylated (17).

Trypanosoma brucei sp., the causative agent of Ngana in ungulates and sleeping sickness in humans, is a parasitic protozoan pathogen seriously affecting public health and the economy in endemic regions. Suramin, a drug currently used in management of African trypanosomiasis, is believed to enter the parasite via endocytosis (18). Resistance to lysis by human serum is mediated by inducible, selective control of endocytosis (19). We can genetically engineer the Rab system to manipulate endocytosis in *T. brucei* and study drug uptake.[1] *T. brucei* additionally provides a convenient model system for elucidation of cell biological processes in a divergent eukaryote with a strongly directional endocytotic/recycling system, where a very small portion of the total membrane (2–3%, Ref. 20) is the site of all endo- and exocytosis. Recycling is very active in *T. brucei*, with more than 95% of endocytosed variant surface glycoprotein (VSG) recycled (21). Here we report on the subcellular location and evolution of three TbRab proteins involved in endocytosis in *T. brucei*.

EXPERIMENTAL PROCEDURES

Trypanosomes—Culture-adapted blood stream form (BSF)[2] *T. brucei*, strain 427, were grown as described (22). Cells were quantitated with a

* This work was supported by Project Grant 051456 from the Wellcome Trust (to M. C. F.) and benefited from equipment grants from the Wellcome Trust (to K. G.). The costs of publication of this article were defrayed in part by the payment of page charges. This article must therefore be hereby marked "*advertisement*" in accordance with 18 U.S.C. Section 1734 solely to indicate this fact.

The nucleotide sequence(s) reported in this paper has been submitted to the GenBank™/EBI Data Bank with accession number(s) AF007547.

§ To whom correspondence should be addressed. Tel.: 44-171-594-5277; Fax: 44-171-594-5207; E-mail: m.field@ic.ac.uk.

[1] H. Field and M. C. Field, unpublished data.

[2] The abbreviations used are: BSF, bloodstream form; EST, expressed sequence tag; FP, flagellar pocket; GST, glutathione *S*-transferase; IFA, immunofluorescence analysis; ISG, invariant surface glycoprotein; kb, kilobase(s); nt, nucleotides; ORF, open reading frame; PAGE, polyacrylamide gel electrophoresis; TLF, trypanosome lytic factor; PCR, polymerase chain reaction; MOPS, 4-morpholinepropanesulfonic acid.

This paper is available on line at http://www.jbc.org

Z2 Coulter Counter (Coulter Electronics, UK). For boiling SDS lysates, freshly harvested trypanosomes were added to SDS-PAGE sample buffer (23) at 95 °C, heated for 10 min, and reduced with dithiothreitol. Treatment with fluorescent endocytotic markers was at 3–4 mg/ml added from 10× stock, in 100 μl of culture medium, with (for Texas red-dextran, Molecular Probes) or without (for Lucifer yellow, Sigma) serum.

Nucleic Acids and Recombinant DNA Methods—Nitrocellulose for Western and Southern blotting was from Schleicher and Schuell, and nylon for Northern blots was from Amersham Pharmacia Biotech. Radioisotopes were from Amersham International, ICN, and NEN Life Science Products. Vector pGEX2tk and glutathione-Sepharose 4B were from Amersham Pharmacia Biotech, and the pQE30 vector and nickel-Sepharose were from Qiagen Inc. Plasmids were grown in *Escherichia coli* XL1-Blue (Stratagene) following transformation by electroporation with a BTX 600 ECM electroporator. PCR products and gel-embedded DNA were purified using PCR cleanup kits (Promega), while plasmid and λ DNA were purified using Qiagen kits following the manufacturer's instructions. Small scale plasmid preparations were performed using the Promega Wizard system. Oligonucleotide primers were obtained from Genosys.

Polymerase Chain Reaction—PCR was performed in 50-μl reactions with 25 pmol of each primer in ammonium buffer (Bioline), 2.5 mM $MgCl_2$, 1 unit of *Taq* polymerase (Bioline) in a 480 thermal cycler (Perkin Elmer) typically as follows: 98 °C, 5 min (1 cycle); 95 °C, 5 min (1 cycle); 94 °C, 1 min; 56 °C, 1 min; 72 °C, 3.5 min (25 cycles). Primers for subcloning and assembling ORFs for expression were: 5BH3 (5′-TCCAAGCTTTCAACCACAGCAACCGGA), 5BKON (5′-CGGGGTAC-CTCTGTGAAGACCGTTGCCG), 5A5′ (5′-CGCGAATTCATATGTCGT-GTCAGCGACACC), and 5A3′ (5′-GAGAGCGGTAGCGCTCCTGCCC).

Southern and Northern Blotting—0.5-μg aliquots of total trypanosome DNA (24) were digested with restriction enzyme, and the fragments resolved on 1% Tris-acetate-EDTA agarose gels. Molecular weights were estimated from comigration of a 1-kb DNA ladder (Life Technologies, Inc.). Filters were prepared by high salt transfer Southern blotting (25) and probed at low (2× SSC, 0.1% SDS, room temperature) or high stringency (0.1× SSC, 0.1% SDS, 65 °C). Poly(A) enriched RNA was isolated (Hybaid Plc), and Northern blot filters were prepared using 20 μg of RNA or RNA from 10^8 trypanosomes/lane, separated on a formamide-MOPS agarose gel in the presence of ethidium bromide followed by transfer in 20× SSC. Molecular weights were estimated from comigration of RNA markers (Life Technologies, Inc.) and trypanosome rRNA species at 1600, 1900, and 2300 bases. Probes were prepared as follows; full-length ORFs from 2 μg of *TbRAB5A, -5B*, or *-4*, and a fragment of tubulin (*Not*I/*Xba*I fragment from pXS2, Ref. 26) were excised and gel-purified. DNA was labeled by random hexamer priming (Boehringer-Mannheim) using 50 μCi [α-^{32}P]dCTP and purified by size exclusion (Centrisep). Autoradiography was with BioMax film (Kodak) at −85 °C with an intensifying screen or by PhosphorImager (Molecular Dynamics). Images were quantitated with NIH Image 1.59 (National Institutes of Health).

DNA Sequencing—Sanger sequencing of the *TbRAB5B* ORF and noncoding region was performed using a deaza-GTP kit (Amersham Pharmacia Biotech) and primer walking in both directions. All other sequence analysis was by dye terminator cycle sequencing on a 377 sequencer (Perkin Elmer) from polyethylene glycol-precipitated DNA (6.5% PEG_{8000}, 0.4 M NaCl on ice 20 min, centrifuged at 13,000 × *g*, 4 °C, 30 min, washed with 70% EtOH).

Isolation of TbRAB5B cDNA and Production of an Expression Construct—cDNA encoding TbRab5Bp was isolated from a *T. brucei* BSF cDNA library in λZAP (gift of Dr. John Mansfield, University of Wisconsin) using *Rtb4* as a probe (27). Screening and recovery of the phagemid was as described (22, 28). The *TbRAB5B* ORF was PCR amplified from the cDNA, engineering a 5′ *Hin*dIII site and a 3′ *Kpn*I site (primers 5BH3, 5BKON). The PCR product was ligated into *Kpn*I/*Hin*dIII-restricted pQE30 (Qiagen Inc.). The construct was verified by sequencing and expression in *E. coli*, producing a 23-kDa protein, the predicted molecular weight for a $(His)_6$·TbRab5Bp fusion.

Construction of a Full-length TbRab5A ORF—The *TbRAB5A* ORF (a gift from Dr. Nabib El-Sayed) was constructed from clone 22, encoding the N terminus of TbRab5Ap,[3] which was PCR amplified (primers 5A5′, 5A3′) to produce overlapping *Eco*RI/*Nde*I sites at the 5′ end and finishing at an existing *Eco*47III site; the PCR product was subcloned and then ligated into *Eco*RI- and *Eco*47III-cleaved clone T378, which encodes the majority of TbRab5Ap in pBluescript (29). The ORF was verified by restriction analysis and sequencing. The plasmid was cleaved with *Xho*I (3′ to the ORF) and blunt ended with Klenow, and the ORF was released with *Bam*HI and ligated into *Bam*HI/*Sma*I-cleaved pGEX-3X (Amersham Pharmacia Biotech) to create an in-frame fusion with glutathione *S*-transferase (GST; a synthetic 4-amino acid linker is present). The construct was verified by expression in *E. coli*, producing a 56-kDa protein, the predicted molecular mass for a GST·TbRab5Ap fusion.

Construction of a Full-length TbRAB4 ORF—The *TbRAB4* ORF (a gift from Dr. Nabib El-Sayed) was constructed from clone 452–5c, encoding the N terminus of TbRab4p,[3] was PCR amplified, producing a 5′ *Eco*RI site and finishing at an existing *Bsa*BI site, and subcloned via these restriction sites directly into clone T452, encoding the majority of TbRab4p in pBluescript (29). The ORF was verified by restriction analysis and sequencing.

Antibodies and Recombinant Proteins—Expression plasmids pGEX-3X·*TbRAB5A* and pQE30·*TbRAB5B* in *E. coli* were grown in L-broth and induced with 0.2–1.0 mM isopropyl-1-thio-β-D-galactopyranoside. GST-TbRab5Ap fusion protein was affinity purified on glutathione-Sepharose 4B as described previously (22, 30); cleavage was with Factor Xa (New England Biolabs) at room temperature for 2 h, adding more enzyme after 1 h. His_6·TbRab5Bp protein was purified on nickel-Sepharose. Protein was estimated by SDS-PAGE and Coomassie staining. Typical yields were 0.4–4 mg of recombinant TbRab protein/liter *E. coli*. Antibodies to TbRab4p, -5Ap, and -5Bp were raised against synthetic peptides designed from the C termini and coupled to bovine serum albumin. Additional residues were included in TbRab4 and -5A peptides, to facilitate detection and derivatization. Peptides WGENG-HAETLYDGPKRFSC (-4), WYGAQRLEPPTRQQKKEGGC (-5A), and ACKGVLGGQPNSTRRSSGC (-5B) were synthesized (Dr. R. Leatherbarrow, Department of Chemistry, Imperial College) and verified for purity by high performance liquid chromatography and for sequence by fast atom bombardment-mass spectrometry, following standard methods. A portion of the peptide was iodinated with IodoBeads (Pierce) or Bolton-Hunter reagent (-5B) and used as a tracer. Peptides were coupled to bovine serum albumin with an efficiency of ~40%, using *m*-maleimidobenzoyl-*N*-hydroxysuccinamide ester (Pierce) following standard procedures (24). The conjugate was used to immunize rabbits and rats using the MPL® + TDM + CWS Adjuvant System (Sigma). Animals were exsanguinated, and serum was stored at 4 °C with azide. For affinity purification, peptide was coupled to either thiol-Sepharose (-5B) or CNBr-Sepharose following the manufacturer's instructions. Antibodies were affinity purified from serum after 50% ammonium sulfate precipitation (31).

Protein Electrophoresis and Western Blotting—Proteins were separated by reducing SDS-PAGE. For Western blots, 5×10^6–2×10^7 cells per lane were electrophoresed on 15% SDS-polyacrylamide minigels and blotted (Amersham Pharmacia Biotech) onto 0.45 μm nitrocellulose. Filters were processed at room temperature. After blocking for 1 h in buffer A (20 mM potassium-Hepes, 2 mM $MgCl_2$, 0.1–1% Tween 20, 110 mM potassium acetate, pH 7.4, containing 2% non-fat milk (Marvel)), filters were washed three times briefly, incubated with primary antibody for 1 h, washed, incubated with horseradish peroxidase-conjugated anti-rabbit antisera at 1:20,000 (Sigma) for 1 h, washed in Buffer A, and then in Buffer A without milk. Visualization was with ECL™ (Amersham Pharmacia Biotech) and x-ray film (Kodak).

GTP Overlay—GTP overlay assay was performed on 10^7 trypanosomes/lane electrophoresed on 15% SDS-polyacrylamide gels (32).

Immunofluorescence Assay—IFA was as described previously (33). BSF and procyclic trypanosomes were washed in phosphate-buffered saline (Sigma), allowed to settle onto poly-lysine coated slides (Sigma) for 3 min (on ice for BSF), fixed in 4% paraformaldehyde (Sigma) in phosphate-buffered saline for 20 min, and then treated with methanol at −20 °C for 5 min. Purified anti-TbRab peptide antibodies were used at 1:50–100 dilution. Secondary antibodies were conjugated with fluorescein isothiocyanate (Sigma), Texas Red, Oregon 488 (Molecular Probes), or Cy3 (Jackson). Cells were examined on a Leica DMRXA epifluorescence microscope fitted with a Photometrics CH250 Slow Scan CCD camera, and digital images were captured using IP Lab Spectrum 3.1. Alternatively, photography was as described (22), with images digitized by scanning photographs (Scanmaker II, Microtek). Resulting images were false-colored, merged, and assembled into figures (Adobe® Photoshop 3.0.5, Adobe® Systems, Inc.) on a MacOS computer (Apple Inc.).

Computer Analysis—Computer analysis was as described (22). Fig. 1 was generated using SEQVU (Garvan Institute of Medical Research, Sidney, Australia).

[3] N. El-Sayed, unpublished data.

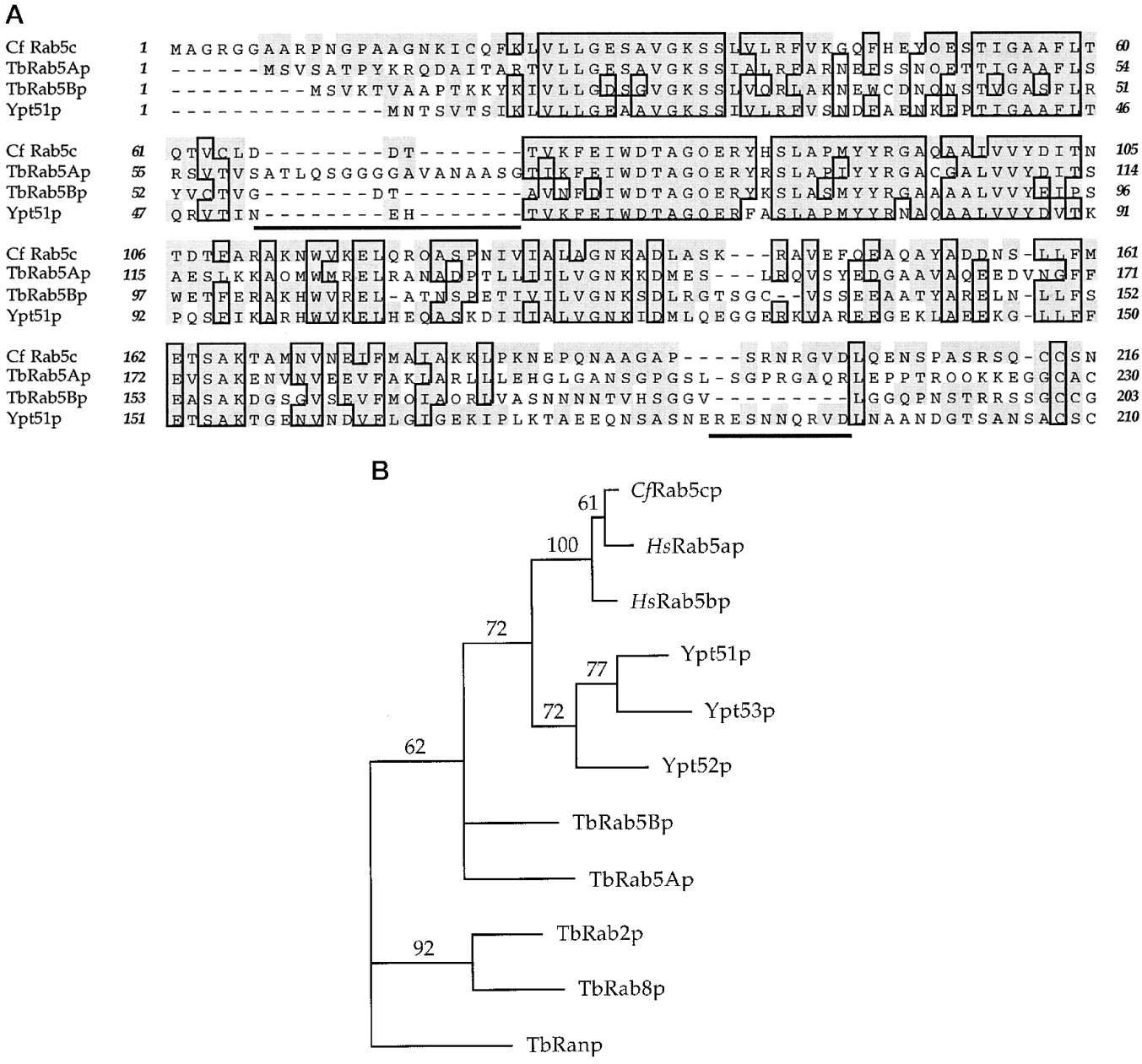

FIG. 1. ***T. brucei* has at least two Rab5 homologues.** *A*, clustal alignment of the hypothetical ORFs of TbRab5Ap and -5Bp from *T. brucei*, together with their closest orthologues from GenBank™. *Boxes* indicate identity and *shading* indicates homology. The indels in TbRab5Ap and -5Bp are *underlined*. *Cf*, *C. familiaris*. *B*, phylogenetic reconstruction using PAUP (43) suggests that Rab5 families have evolved several times. TbRab5Ap and -5Bp were examined in relation to protein homologues representative of sequences from all three mammalian Rab5 subclasses and the three yeast Ypt5s. Rab5 sequences from the same order emerge as monophyletic, suggesting that divergence of the mammalian, fungal, and trypanosomatid lineages predates emergence of multiple Rab5 isoforms. The tree was obtained from 1000 branched and bound bootstrap replicates after a branched and bound search. *Cf*, *C. familiaris*; *Hs*, *H. sapiens*; *Ypt*, *S. cerevisiae*; *Tb*, *T. brucei.* Ran/TC4 was chosen as an outgroup, and monophyletic TbRab2p/-8p were included as a control. *Numbers* are percent confidence for various branch points following bootstrapping. *Horizontal distances* represent relative genetic distance.

RESULTS

Isolation of cDNA of a Second T. brucei Rab5 Homologue—A *T. brucei* homologue of mammalian Rab5 was previously isolated (T.b. Rab5, Ref. 29); we designate it TbRab5Ap. A second Rab5 homologue was identified in *T. brucei* by reverse transcriptase PCR using a degenerate primer to the WDTAGQE motif of Rab GTPases. An EST, *Rtb4* (27), was used to probe a *T. brucei* BSF cDNA library. A full-length cDNA of ~2.0 kb was cloned and sequenced. The ORF was hypothetically translated and identified as a Rab5 homologue (Fig. 1*A*) by BLAST search of GenBank™ and designated TbRab5Bp. Neither *T. brucei* Rab5 clearly corresponded to a particular Rab5 subclass.

Comparison of TbRab5Bp with -5Ap and other Rab5 protein sequences (Fig. 1*A*, and Table I) confirmed the conservation of canonical Rab protein features, *i.e.* GTP-binding regions, effector loops, and dicysteinyl C-terminal isoprenylation signal (34), but two differences were seen between TbRab5Ap and -5Bp. The first is an insertion in TbRab5Ap (residues 61–77) with a high Ala and Gly content; this region corresponds to a loop between β-sheets 2 and 3 in the Ras structure and is predicted to be on the protein surface and highly mobile. The second is a deletion in -5Bp within the hypervariable region (Fig. 1*A*); this is more common as similar but smaller indels are found in this region of mammalian Rab5 s and TbRab5Ap when compared with Ypt51p, -52p, and -53p (not shown).

Phylogenetic Reconstruction of the Rab5 Lineage—By BLAST

TABLE I
Homology between TbRab5Ap, −5Bp, and closest homologues in the data base

The hypothetical translations of the *TbRAB5A* and *−5B* ORFs were used to search GenBank.℠ The top scoring match is shown in each case. Values above the diagonal are percent similarity and below percent identity.

	Rab5c *C. familaris*	Ypt51p *S. cerevisiae*	TbRab5Ap	TbRab5Bp
Rab5c		72.7	64.6	63.4
Ypt51p	52.5		65.5	61.6
TbRab5Ap	44.0	47.1		63.3
TbRab5Bp	47.0	41.9	45.2	

search, the nearest homologue of TbRab5Ap was Ypt51p and of -5Bp was *Canis familiaris* Rab5c (Table I). TbRab5Ap and -5Bp were as similar to each other as to their nearest homologues (Table I) so could not be assigned to specific Rab5 subgroups. A phylogeny for the Rab5 lineage was constructed, using Clustal (4.0) followed by PAUP, on sequences representative of the subclasses of Rab5 so far identified in mammals (Rab5a, -5b, and -5c) and the three Rab5 homologues from *Saccharomyces cerevisiae* (Ypt51p, -52p, and -53p). Rab5 proteins from any one of the three lineages were monophyletic (Fig. 1*B*). The simplest interpretation of this topology is that proliferation of the Rab5 subclasses occurred after speciation and that a single progenitor Rab5 gene was present in the eukaryote common ancestor.

Genomic Organization—Because TbRab5Ap and -5Bp are closely related, we asked whether the genes encoding them (*TbRAB5A* and *-5B*) were linked in the genome. Trypanosome genomic DNA, digested with a panel of restriction enzymes, was Southern blotted and probed with the complete ORFs of *TbRAB5A* and *-5B* (Fig. 2*A*). No cross-hybridization between probes was detected using plasmids as targets at low stringency (not shown). There was no coincidence between the hybridization patterns obtained with *TbRAB5A* and *-5B*, reflected in the different maps obtained for the two genes (Fig. 2*B*).

The *TbRAB5B* probe revealed the presence of a restriction fragment-length polymorphism (Fig. 2*B, asterisk*) giving a doublet in *Sac*II digests although previous Southern blot analysis of the trypanosome genome with the *Rtb4* probe (the 5′ third of the *-5B* ORF) suggested that *TbRAB5B* was single copy (27). In our original EST study, we isolated a second partial cDNA (*Rtb9*) closely related to *Rtb4* but with a small number of substitutions (27). These data suggest that *Rtb4* and *Rtb9* are derived from allelic copies of *TbRAB5B*.

There was no additional hybridization with the *TbRAB5A* or *-5B* probes. As these two probes do not cross-hybridize at low stringency, there are no sequences more closely related to *TbRAB5A* than *-5B* and *vice versa* in the trypanosome genome, but more distantly related *TbRAB5* genes may have been undetectable and therefore cannot be formally excluded. Southern analysis with the *TbRAB4* ORF revealed a single copy, with no evidence for linkage between *TbRAB4* and any other *TbRAB* gene so far studied (Fig. 2*A*, Ref. 27).

Expression of TbRAB Genes—Poly(A)-enriched RNA from 10^8 trypanosomes (3.4 μg from BSF and 10 μg from procyclics: the differing RNA yield is a known phenomenon[4]) was used in each lane of a Northern blot and probed with ORFs from *TbRAB4*, *-5A*, and *-5B* (Fig. 3). *TbRAB4* detected a single major species migrating at ~0.7 kb, with the ORF of 718 nt suggesting minimal untranslated sequence (UTR), and *TbRAB5A* detected a single species of ~1.0 kb, with the ORF of 930 nt so there is again very little UTR. In contrast, *TbRAB5B* detected larger message species. As the 5′ UTR is 150 nt and the ORF 612 nt, the 3′ UTR is ~1.2 kb and could potentially include regulatory sequences. The message levels were at a ratio of ~10:20:1 for TbRab4:-5A:-5B, with -5B particularly difficult to detect because of low abundance and molecular weight heterogeneity, differing in BSF (3.8, 2.4, 2.1*, 1.8, 1.35 kb) and procyclics (3.8*, 2.3, 1.95* kb, where asterisks indicate the prominent message sizes). The 3.8-kb message probably represents an unprocessed nuclear transcript. The 2.0-kb cDNA clone containing *TbRAB5B* is consistent with a message size of 2.1–2.4 kb.

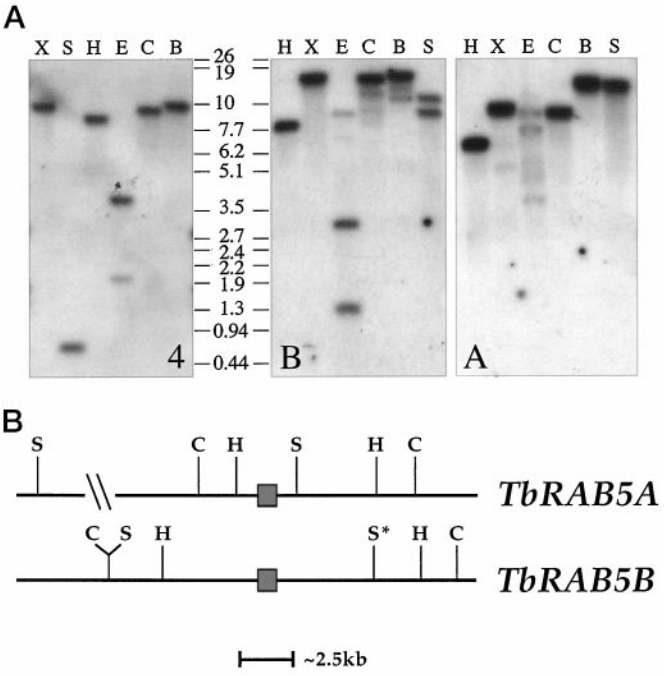

FIG. 2. **Genomic organization of *TbRAB5A* and *-5B* indicates absence of linkage.** *A*, Southern blots probed with *TbRAB4* (*panel 4*), *-5A* (*panel A*), and *-5B* (*panel B*) ORFs. Genomic DNA from *T. brucei* was digested with restriction enzymes *Bam*HI (*B*), *Cla*I (*C*), *Eco*RI (*E*), *Hin*dIII (*H*), *Sac*II (*S*), or *Xho*I (*X*). Markers are in kilobases. For *TbRAB5A* and *-5B*, star activity resulted in overdigestion by *Eco*RI; in other experiments bands were obtained at ~12 kb (*-5A* and *-5B*). *B*, restriction maps of the *TbRAB5A* and *-5B* genes as determined by Southern analysis. Total trypanosome DNA was single (*Panel A*) or double-digested (not shown) with *Cla*I (*C*), *Hin*dIII (*H*), and *Sac*II (*S*). *Asterisk* indicates a *Sac*II RFLP in *TbRAB5B*.

For quantitation, the blots were reprobed with tubulin as a constitutively expressed standard; the signal intensity was at ~1:4 for BSF:procyclics and ~1:1 with the mass of RNA loaded. When normalized to tubulin, both TbRab4 and -5A messages were constitutive. The 3.8-kb TbRab5B message is also constitutive; conversely the ~1.8–2.4-kb -5B transcripts normalized to tubulin at a ratio of 1:0.5, indicating more processed -5B message in BSF than in procyclics. In separate experiments loading equal masses of BSF and procyclic poly(A)-enriched RNA or poly(A)-selected RNA, hybridization signals for *TbRAB5B* were more intense in BSF, confirming that TbRab5Bp is developmentally regulated[5] (Ref. 27).

GTPase activity was assessed in the two life stages by GTP overlay of lysates from 10^7 BSF or procyclic cells (Fig. 4). Total protein levels are approximately equal for both BSF and procyclic cells (Fig. 4).[1] The pattern of GTP-bound bands was essentially identical, while significantly more GTP was bound

[4] J. Boothroyd, personal communication.

[5] H. Field, A. Pal, and M. C. Field, unpublished data.

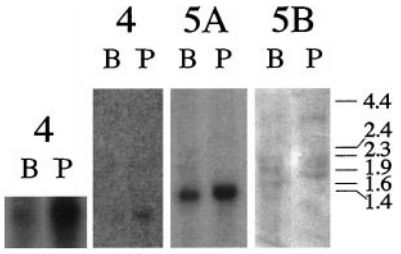

FIG. 3. **Developmentally regulated expression of *TbRAB5B* but not *-5A* or *-4*.** Northern blot analysis of poly(A)-enriched RNA extracted from 10^8 BSF (*B*) or procyclic form (*P*) *T. brucei*. Identical blots were probed with the ORFs of *TbRAB4*, *-5A,* and *-5B* and washed at low and high stringency. Molecular weights are in kilobases. *Left-most lanes* are TbRab4 probed at low stringency, and the remainder are at high stringency. The same blots were reprobed with tubulin (not shown), and the ratio of message in BSF compared with procyclic cells was determined for each message (see text). TbRab5B mRNA is more abundant in BSF than procyclic when normalized to tubulin, whereas -4 and -5A messages are found at approximately equal levels in both life stages.

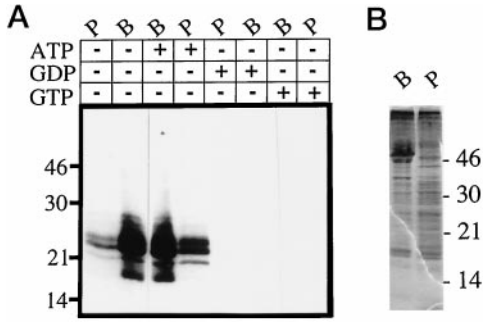

FIG. 4. **Total small G protein activity is increased in BSF compared with procyclic cells.** *A*, ligand blot analysis of total GTP-binding proteins in BSF (*B*) and procyclic (*P*) *T. brucei*. Boiling SDS lysates were prepared (10^7 cells/lane), fractionated by reducing SDS-PAGE, renatured, transferred to nitrocellulose, and overlaid with [^{32}P]GTP in a solution containing ATP. *Control lanes* were co-exposed to excess unlabeled GTP, GDP, or ATP. GTP-binding activity is recovered in the 17–30 kDa range and is ~10-fold greater in the BSF. Longer exposure confirms that the pattern of bands is similar in procyclic and BSF cells (not shown). The experiment has been repeated four times with essentially identical results. *B*, Coomassie-stained proteins from two lanes of the gel used for *panel A* showing equivalent loading in BSF (*B*) and procyclics (*P*). Marker sizes are shown in kDa.

by BSF lysate than procyclic.

Production and Characterization of Specific Antisera to TbRab4p, -5Ap, and -5Bp—Rat (anti-TbRab4p and -5Ap) and rabbit antisera (-5Bp) were raised against synthetic peptides corresponding to the C termini of the TbRab sequences and affinity purified, and the specificity of anti-TbRab5Ap and -5Bp sera were checked by Western blotting against lysates of *E. coli* overexpressing recombinant TbRab (Fig. 5*A*). Anti-TbRab5Ap recognized recombinant -5Ap but not -5Bp, and *vice versa*. No signal was observed using anti-TbRab4p or -5Ap antibodies in Western blotting on trypanosome lysates (Fig. 5*B*, and data not shown). Extra residues added to the TbRab5Ap and -4p peptides may explain their relative lack of reactivity in Westerns, but inactivity in Western blotting is commonly observed for anti-Rab C-terminal peptide antibodies that work well in IFA (35) and for antipeptide antibodies in general. Antibodies to TbRab5Bp reacted against two bands at 24 and 17 kDa. The TbRab5B protein is 21.8 kDa and is expected to be doubly geranylgeranylated so probably corresponds to the 24-kDa band. The 17-kDa band is most likely a degradation product because it was also detected by Western blotting in some *E. coli* lysates.

Immunolocalization of TbRab4p, -5Ap, and -5Bp—Based on

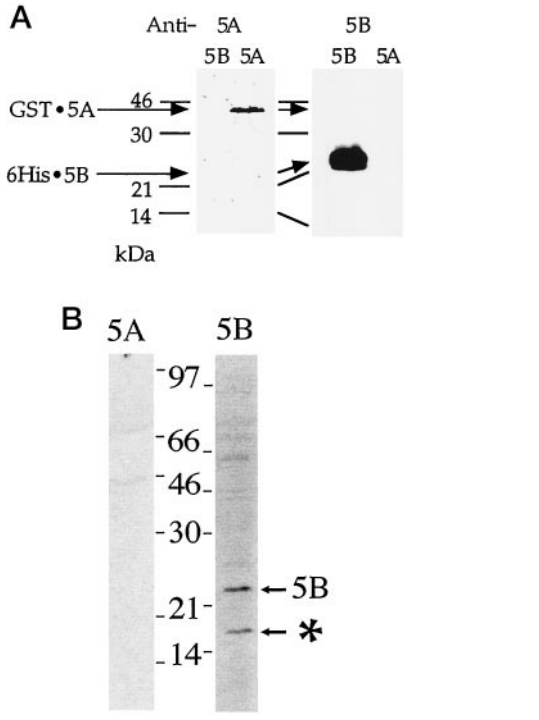

FIG. 5. **Characterization of affinity-purified antisera to TbRab5Ap and -5Bp.** *A*, antipeptide antibodies affinity purified from rat (anti-TbRab5Ap, at 1:100) or rabbit (anti-5Bp, at 1:300) sera were used to probe Western blots prepared from lysates of *E. coli* strains expressing recombinant GST-TbRab5Ap and $(His)_6$-TbRab5Bp. Detection was with ECL™ (Amersham Pharmacia Biotech) for 1–5 min. *B*, Western blots of 10^7 trypanosomes/lane, with rabbit anti-TbRab5Ap antibodies at 1:20 dilution, or anti-TbRab5Bp antibodies at 1:200 dilution. Wild type TbRab5Bp is detectable in trypanosomes at 24 kDa; a 17-kDa band (*asterisk*) is probably a degradation product (see "Results"). Detection was with ECL™.

sequence similarity, it is most probable that the TbRab4p, -5Ap, and -5Bp are trypanosome homologues of Rab4 and Rab5. To confirm that that these proteins are components of the trypanosome endosomal system, we determined the location of the TbRab proteins. All three antibodies recognized a large number of vesicular structures in the trypanosome cytoplasm.

Staining for both TbRab5Ap and -5Bp produced very similar patterns with small vesicular structures concentrated at high density between the nucleus and kinetoplast in interphase cells, suggesting that the majority of TbRab5 compartments were located closer to the FP which is consistent with an active role in endocytosis (Fig. 6*A*). Indeed, the similarity of the staining was highlighted by colabeling of cells for both TbRab5Ap and -5Bp; this demonstrated that the vast majority of the vesicles contained both proteins, with only a small subpopulation bearing only one of the TbRab5 s (Fig. 6*A*). No obvious difference was seen between procyclic and BSF (Fig. 6, *A–C*). Interestingly, in mitotic cells we found that the TbRab5Ap/-5Bp compartment migrated from the posterior region of the cell to a position anterior to the nucleus (Fig. 6*B*). The repositioning occurred as the kinetoplast divided (not shown).

To confirm that TbRab5Ap and -5Bp were indeed located on compartments associated with the trypanosome endocytic system, we costained BSF cells with antibodies to TbRab5p and ISG_{100}, a recently characterized cell surface protein that is also present throughout the endosomal system including the lysosomes (36). The majority of ISG_{100} colocalized with TbRab5Bp, particularly in a number of vesicles between the kinetoplast and the nucleus (Fig. 6*C*, *arrowheads*). These data, taken together with the high degree of sequence relatedness, confirm TbRab5Ap and TbRab5Bp as Rab5 homologues positioned at

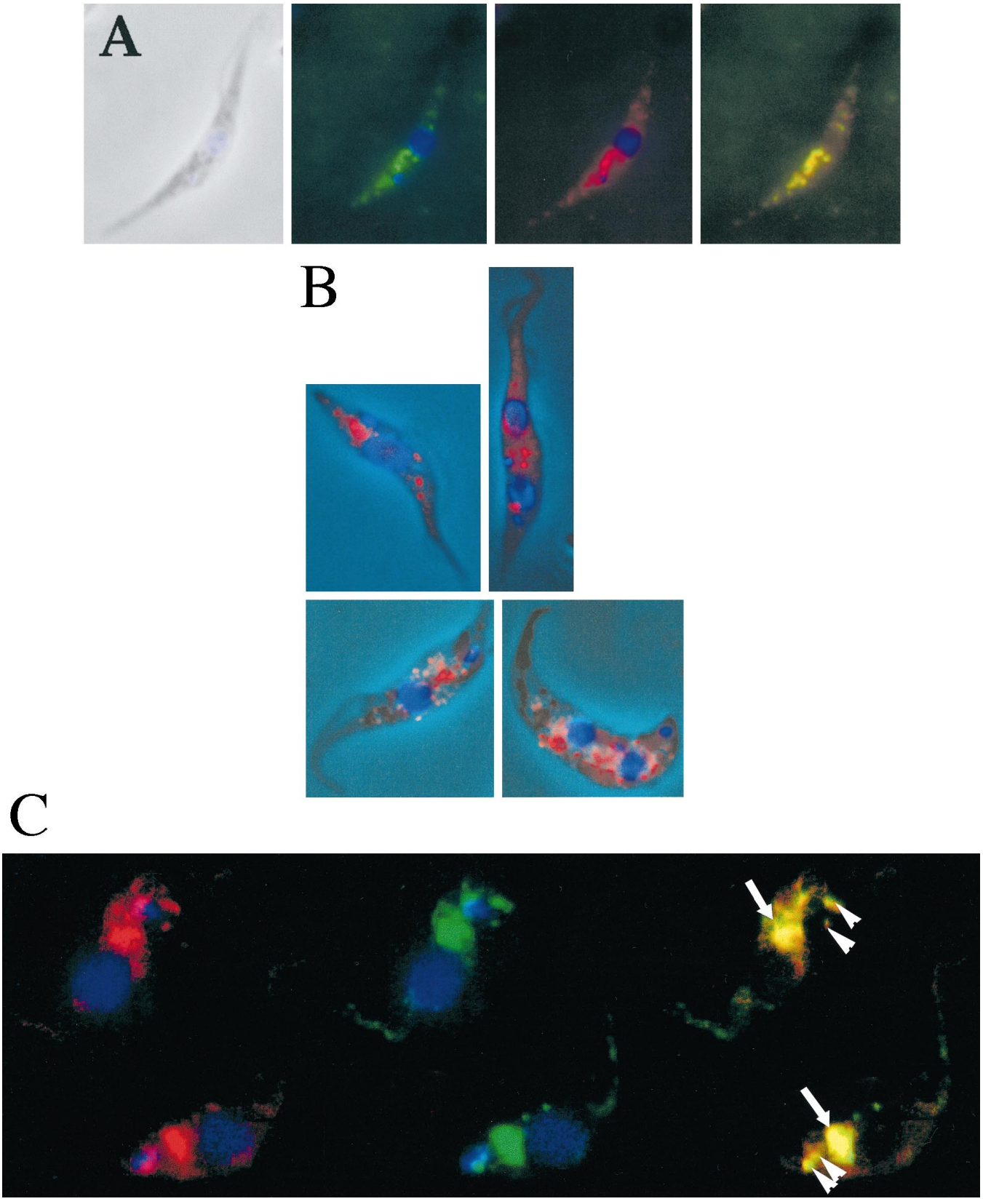

FIG. 6. **TbRab5Ap and -5Bp are associated with endosomal compartments.** Immunofluorescence analysis of procyclic and BSF trypanosomes. *A*, procyclic trypanosome stained for DNA (*blue*), TbRab5Ap (*green*), and -5Bp (*red*). Phase contrast images of the cell (*right*) and merged fluorescence is shown (*left*, coincident staining is *yellow*). Note the significant, but not complete, coincidence of staining for the two Rab5 s. *B*, reorganization of the TbRab5Ap (*top*) and -5Bp (*lower*) compartment during mitosis in procyclics. Interphase (*left*) and corresponding mitotic cells (*right*) are shown. DNA (*blue*) and TbRab5 stain (*red*) are overlaid onto phase contrast images of the cell, with the kinetoplast (small) at the posterior end of the cell. In interphase cells, the majority of TbRab5p staining is between the kinetoplast and the nucleus whereas in the mitotic cell most TbRab5p is anterior of the respective nucleus. *C*, BSF trypanosome stained with antibodies to TbRab5Bp (*red*), ISG_{100} (*green*), and DNA (*blue*). *Right-most panel* shows merged fluorescence data with coincident staining in *yellow*. *Arrowheads* indicate some of the endosomal vesicle structures where there is coincident staining. ISG_{100} stain is mainly in lysosomal structures in this example, as previously reported (*arrows*).

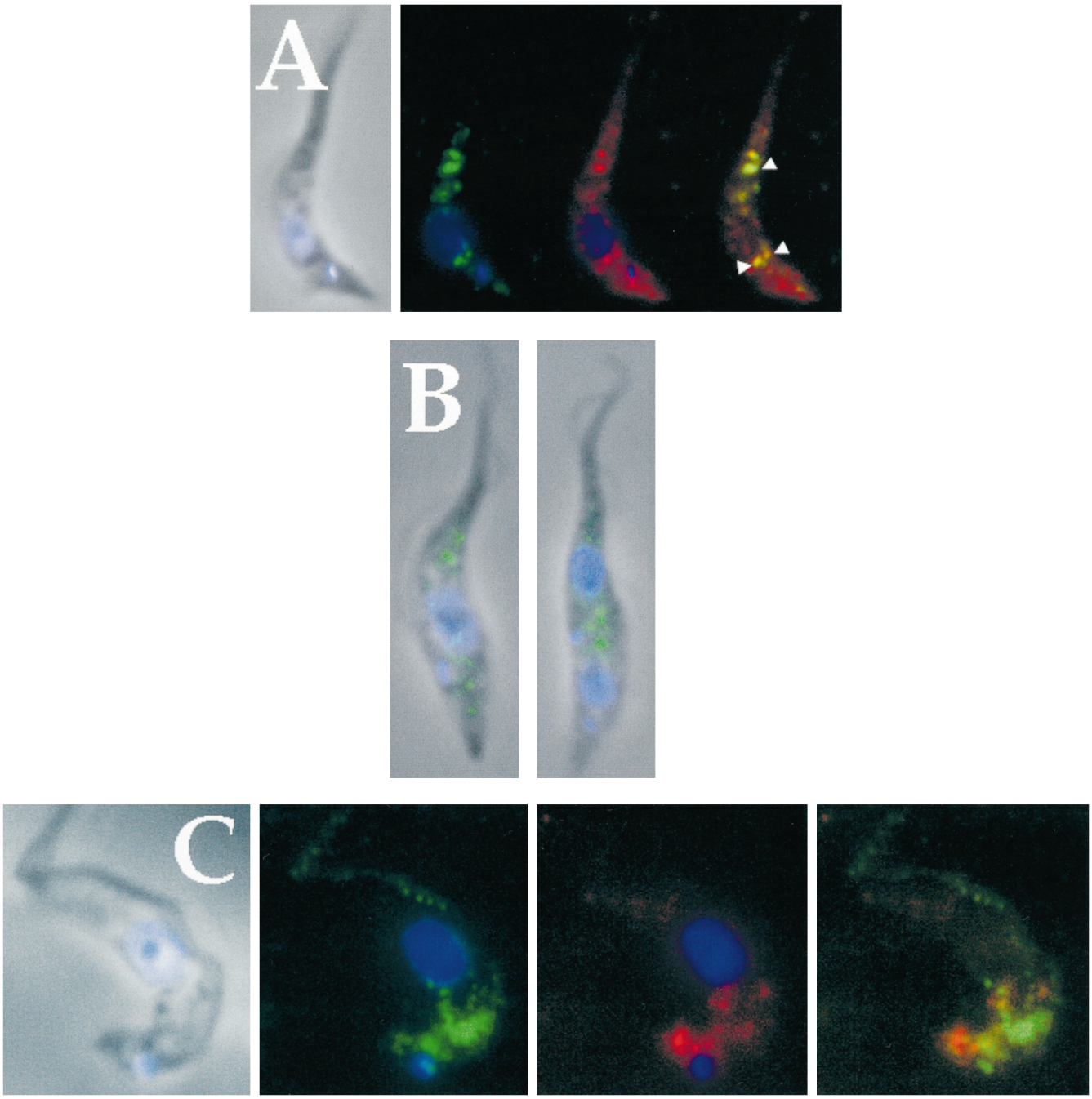

FIG. 7. **TbRab4p is associated with early endocytotic vesicles.** *A*, procyclic form trypanosome stained for DNA (*blue*), TbRab4p (*green*), and TbRab5Bp (*red*). Phase contrast image of the cell (*right*) and merged fluorescence is shown (*left*, coincident staining is *yellow*). *Arrowheads* indicate positions of coincident staining for TbRab4p and -5Bp. Most of the staining does not overlap. *B*, TbRab4p (*green*) location in interphase (*left*) and mitotic procyclic cells (*right*), TbRab4p stain (*green*), and DNA (*blue*) is overlaid onto phase contrast images of the cell, positioned with the kinetoplast (small *blue* structure) at the bottom. Note a similar migration to the anterior pole of the cell as for TbRab5A/-5Bp, with the exception that in interphase there are already greater numbers of TbRab4p vesicles in the cell anterior. *C*, BSF stained for DNA (*blue*), ISG_{100} (*green*), and TbRab4p (*red*). Phase contrast images of the cell (*right*) and merged fluorescence is shown (*left*, coincident staining is *yellow*). Essentially no colocalization is seen for the two proteins.

endocytotic structures. In addition, the similarity of the staining in *panel B* (procyclic cells) compared with *panel C* (BSF) confirms the presence of endocytic structures in both life stages; TbRab5Ap staining in BSF cells (not shown) is likewise similar to that of procyclics (Fig. 6, *A* and *B*).

TbRab4p antibodies recognized numerous small compartments throughout the cell in both procyclic and BSF trypanosomes (Fig. 7). A small amount of colocalization with TbRab5Bp (Fig. 7*A*) and -5Ap (not shown) was detected, suggesting that TbRab4p is also a component of the endosomal system, but is distinct from the majority of the TbRab5p compartment. Similar to TbRab5p, we also observed a migration during mitosis to an anterior position (Fig. 7*B*). TbRab4p mostly did not colocalize with ISG_{100} (Fig. 7*C*), confirming the separate identity of the Rab4 compartment. These data are consistent with that expected for a Rab4 homologue involved in recycling (37) and, with the sequence similarity (29), show TbRab4p to be a functional trypanosome Rab4. Again, comparison of procyclic and BSF (Fig. 7) demonstrates the constitutive presence of the TbRab4p compartment. Therefore, in trypanosomes as in mammals, the endosomal system is divided between an endosomal compartment controlled by functionally

redundant Rab5 homologues and a separate recycling system communicating with the endosomal pathway and governed by a Rab4 homologue.

DISCUSSION

We show here that the endosome system of the African trypanosome has multiple Rab5 isoforms. The two TbRab5 protein sequences, TbRab5Ap (29) and TbRab5Bp (this report), are clearly distinct; divergence is most apparent in the occurrence of insertions in the center of the molecule and within the hypervariable C-terminal region. Southern analysis demonstrated that *TbRAB5A* and *-5B* genes are not closely linked in the trypanosome genome, so emergence of these two isoforms has been via duplication followed by genomic rearrangement. This is distinct from two other *T. brucei* Rab genes, *TbRAB2* and *TbRAB8*, which arose by tandem duplication but have not separated (22). Southern blotting also revealed a restriction fragment length polymorphism in *TbRAB5B*, and the second allele probably encodes EST *Rtb9* (27).

TbRab4p, 5Ap, and -5Bp are all associated with the endocytotic pathway as demonstrated by IFA, costaining with specific anti-peptide antibodies and anti-ISG_{100} antibodies. The compartments recognized by these antibodies indicates that the endocytotic network is extensive and present in both life forms even though endocytosis is not an active process in procyclics. The inter-nucleo-kinetoplast region of the cell contains the FP and is the primary site of endocytotic activity, as visualized by Lucifer yellow (a fluid phase endocytosis marker[1]) or TR-dextran uptake (19). This is also the region where anti-TbRab5Ap, -5Bp, and ISG_{100} staining is most concentrated. TbRab4p-containing vesicles are also located anterior of the nucleus, in contrast to TbRab5p vesicles. There is also very little colocalization between TbRab4p and TbRab5p although the majority of the two TbRab5 proteins are present on the same vesicle population. We have shown that the Golgi apparatus is found in the inter-nucleo-kinetoplast region, posterior and adjacent to the nucleus (22),[6] and would be expected to recycle components to and from the endocytotic pathway.

The different patterns for TbRab4 and TbRab5 proteins demonstrate specific subpopulations of vesicles consistent with a complex endosomal system similar to that of higher eukaryotes. The observation of identical staining patterns for TbRab5 homologues suggests that, as in mammalian and yeast systems, the Rab5 compartment is one entity. This division into Rab5 and Rab4 compartments suggests that the trypanosomal endocytotic system is more like that of mammals than that of yeast, where a Rab4 homologue has not been specifically designated (10). To confirm that TbRab5Ap and -5Bp are localized on completely overlapping populations of vesicles, and because of the difficulty of resolving small vesicles in trypanosomes at the light microscopy level, we are producing transgenic trypanosomes overexpressing wild-type and mutant forms of the TbRab proteins to alter endosome size and are addressing this question directly.

We speculate that the reorientation of the TbRab5p and TbRab4p endosome systems from posterior to anterior of the nucleus during cell division may play a role in cell-cycle-dependent plasma membrane events and suggest that the TbRab4p and TbRab5p compartments are under coordinate control, presumably by cytoskeletal elements. Movements of the kinetoplast and basal body during the cell cycle are microtubule-driven (38) and endosome maturation is also microtubule-dependent (39). These data suggest that during cytokinesis, movement of membrane-bound organelles, specifically endosomes, the kinetoplast, basal body, and Golgi apparatus,[6] is coordinated by microtubules and possibly other cytoskeletal elements, ensuring accurate partitioning to the daughter cells.

Northern blots suggest developmental regulation of the TbRab5B message, which is more abundant in the BSF. In contrast, the TbRab5A and TbRab4 messages are constitutive compared with tubulin. As well as being stage specifically up-regulated, the TbRab5B message has an extended 3′UTR compared with the -5A and -4 messages, which have virtually no UTR sequence. The TbRab5B message is clearly expressed at much lower levels than the -5A message, indicating that TbRab5Ap is more abundant than -5Bp although this was not tested at the protein level. This suggests that the putatively more abundant TbRab5Ap may do the bulk of the work in promoting targeting and fusion in endocytosis, whereas TbRab5Bp, expressed at low levels, is implicated in the regulatory control of endocytotic levels between the two life stages. Procyclic cells do not endocytose markers such as TR-dextran which are taken into the BSF within minutes (40). Endocytotic activity therefore correlates with TbRab5B message levels and may be related to differential message processing observed between BSF and procyclic cells. This is the first observation of developmental regulation of TbRab protein expression and suggests that TbRab5Bp is an important component of parasite life-stage developmental response to different environments. The rate of endocytosis is also seen to be related to Rab4 and Rab5 expression in hepatocytes (41). This has general implications for these small G proteins as important regulators of the cell's response to altered environment.

A model where one Rab5 does the work and a second Rab5 is responsible for stage-specific regulation is consistent with the situation in *S. cerevisiae*, where the more abundant Ypt51p is essential for transport of secreted proteins, whereas Ypt52p and Ypt53p appear redundant and the genes without phenotype when deleted (8, 10). Our analysis represents the first functional dissection of a multiprotein Rab5 family, because in the yeast and mammalian systems there is no proposed role for the apparent redundancy in the Rab5/Ypt5p systems. Interestingly, endocytosis may be stimulated in procyclics by overexpression of a secretory Rab protein causing an increase in fluid phase marker (Lucifer yellow) uptake, correlating with the appearance of clathrin coated pits[1], suggesting that the components required for endocytosis are latent within the procyclic cell, consistent with our observations of TbRab4p, -5Ap, and -5Bp in both life stages.

Qualitative differences in endocytosis are particularly dramatic for *T. brucei* spp. *T. brucei brucei* is lysed by human serum because it actively endocytoses from human serum a lytic factor (TLF, a haptoglobin-related component of high density lipoprotein), whereas *T. brucei rhodesiense*, normally resistant to human serum can become sensitive to TLF during serial passage through mice, because specific endocytosis of this factor is no longer suppressed (19). Procyclic *T. brucei brucei* are resistant because of their complete inability to endocytose exogenous TLF. Lysis of BSF *T. brucei* by tumor necrosis factor α is likewise dependent on endocytosis of the cytokine (42), and there is increased sensitivity to lysis by tumor necrosis factor α in trypanosomes at high parasitemia compared with trypanosomes at lower cell densities. These observations clearly imply that manipulation of endocytosis by the trypanosome is stage-specific and is a potential virulence mechanism.

Acknowledgments—We most gratefully acknowledge the generous gifts of the cDNAs encoding *TbRAB4* and *-5A* from Drs. J. Donelson and N. El-Sayed, the cDNA library from Dr. J. Mansfield, and antibodies against ISG_{100} from Dr. D. Nolan. We are also grateful to the following people for contributions to portions of this work: K. Strisovsky for

[6] H. Field, T. Sherwin, K. Gull, and M. C. Field, submitted for publication.

affinity purification of TbRab5Bp antisera, Dr. T. Sherwin for assistance with IFA, Drs. R. Leatherbarrow and G. McBride for peptide synthesis and high performance liquid chromatography, and Prof. A. Dell for fast atom bombardment-mass spectrometry. We also thank the members of our laboratories for helpful discussion and reading of the manuscript.

REFERENCES

1. Novick, P., and Brennwald, P. (1993) *Cell* **75,** 597–601
2. Chavrier, P., Gorvel, J. P., Stelzer, E., Simons, K., Gruenberg, J., and Zerial, M. (1991) *Nature* **353,** 769–772
3. Steele-Mortimer, O., Clague, M. J., Huber, L. A., Chavrier, P., Gruenberg, J., and Gorvel, J.-P. (1994) *EMBO J.* **13,** 34–41
4. Pfeffer, S. R. (1996) *Annu. Rev. Cell Dev. Biol.* **12,** 441–461
5. Lupashin, V. V., and Waters, M. G. (1997) *Science* **276,** 1255–1258
6. Rybin, V., Ullrich, O. Rubino, M., Alexandrov, K., Simon, I., Seabra, M. C., Goody, R., and Zerial M. (1996) *Nature* **383,** 266–269
7. Bucci, C., Lutcke, A., Steele-Mortimer, O., Olkkonen, V. M., Dupree, P., Chiariello, M., Bruni, C. B., Simons, K., and Zerial, M. (1995) *FEBS Lett.* **366,** 65–71
8. Singer-Kruger, B., Stenmark, H., Dusterhoft, A., Philippsen, P., Yoo, J. S., Gallwitz, D., and Zerial, M. (1994) *J. Cell Biol.* **125,** 283–298
9. Singer-Kruger, B., Stenmark, H., and Zerial, M. (1995) *J. Cell Sci.* **108,** 3509–3521
10. Lazar, T., Götte, M., and Gallwitz, D. (1997) *Trends Biochem. Sci.* **22,** 468–472
11. Stenmark, H., Parton, R. G., Steele-Mortimer, O., Lutcke, A., Gruenberg, J., and Zerial, M. (1994) *EMBO J.* **13,** 1287–1296
12. Barbieri, M. A., Li, G., Mayorga, L. S., and Stahl, P. D. (1996) *Arch. Biochem. Biophys.* **326,** 64–72
13. Li, G., D'Souza-Schorey, C., Barbieri, M. A., Roberts, R. L., Klippel, A., Williams, L. T., and Stahl, P. D. (1995) *Proc. Natl. Acad. Sci. U. S. A.* **92,** 10207–10211
14. Van Der Sluijs, P., Hull, M., Zahraoui, A., Tavitian, A., Goud, B., and Mellman, I. (1991) *Proc. Natl. Acad. Sci. U. S. A.* **88,** 6313–6317
15. Bailly, E., McCaffrey, M., Touchot, N., Zahraoui, A., Goud, B., and Bornens, M. (1991) *Nature* **350,** 715–718
16. Shibata, H., Omata, W., and Kojima, I. (1997) *J. Biol. Chem.* **272,** 14542–14546
17. Bucci, C., and Zerial, M. (1995) *Guidebook to the Small GTPases* (Zerial, M., and Huber, L. A., eds) pp. 324–326, Oxford University Press, Oxford, UK
18. Wang, C. C. (1995) *Annu. Rev. Pharmacol. Toxicol.* **35,** 93–127
19. Hager, K. M., and Hajduk, S. L. (1997) *Nature* **385,** 823–826
20. Webster, P., and Russell, D. G. (1993) *Parasitol. Today* **9,** 201–206
21. Duszenko, M., and Seyfang, A. (1993) *Advances in Cell and Molecular Biology of Membranes* (Tartakoff, A. M., and Plattner, H., eds) pp.227–258, JAI Press Inc., CT
22. Field, H., and Field, M. C. (1997) *J. Biol. Chem.* **272,** 10498–10505
23. Laemmli, U. K. (1970) *Nature* **227,** 680–685
24. Medina-Acosta, E., and Cross, G. A. M. (1993) *Mol. Biochem. Parasitol.* **59,** 327–330
25. Ausubel, F. M., Brent, R., Kingston, R. E., Moore, D. D., Seidman, J. G., Smith, J. A., and Struhl, K. (1994) *Current Protocols in Molecular Biology*, Wiley Interscience, New York
26. Bangs J. D., Brouch, E. M., Ransom, D. M., and Roggy, J. L. (1996) *J. Biol. Chem.* **271,** 18387–18393
27. Field, M. C., and Boothroyd, J. C. (1995) *Exp. Parasitol.* **81,** 313–320
28. Field, M. C., Field, H., and Boothroyd, J. C. (1995) *Mol. Biochem. Parasitol.* **69,** 131–134
29. El-Sayed, N. M. A., Alarcon, C. M., Beck, J. C., Sheffield, V. C., and Donelson, J. E. (1995) *Mol. Biochem. Parasitol.* **73,** 75–90
30. Ridley, A. J., and Hall, A. (1992) *Cell* **70,** 389–399
31. Harlow, E., and Lane, D. (eds) (1988) *Antibodies, a Laboratory Manual*, Cold Spring Harbor Laboratory, Cold Spring Harbor, NY
32. Wilson, A. L., Sheridan, K. M., Erdman R. A., and Maltese, W. A. (1996) *Biochem. J.* **318,** 1007–1014
33. Sherwin, T., and Read, M. (1993) *Methods Mol. Biol.* **21,** 407–414
34. Seabra, M. C., Goldstein, J. L., Sudhof, T. C., and Brown, M. S. (1992) *J. Biol. Chem.* **267,** 14497–14503
35. Zerial, M., Parton, R., Chavrier, P., and Frank, R. (1992) *Methods Enzymol.* **219,** 398–407
36. Nolan, D. P., Jackson, D. G., Windle, H. J., Pays, A., Geuskens, M., Michel, A., Voorheis, H. P., and Pays, E. (1997) *J. Biol. Chem.* **272,** 29212–29221
37. Mellman, I. (1996) *Ann. Rev. Cell Dev. Biol.* **12,** 575–625
38. Robinson, D. R., and Gull, K. (1991) *Nature* **352,** 731–733
39. Nelson, W. J. (1991) *Semin. Cell. Biol.* **2,** 375–385
40. Hajduk, S. L., Hager, K. M., and Esko, J. D., (1994) *Annu. Rev. Microbiol.* **48,** 139–162
41. Juvet, L. K., Berg, T., and Gjoen, T. (1997) *Hepatology* **25,** 1204–1212
42. Magez, S., Geuskens, M., Beschin, A., Favero, H., Verschueren, H., Lucas, R., Pays, E., and de Baetselier, P. (1997) *J. Cell Biol.* **137,** 715–727
43. Swafford, D. L. (1993) *Phylogenetic Analysis Using Parsimony*, Version 3.1.1, Illinois History Survey, Champaign, IL